International Current Journal of Engineering and Science (ICJES)
Volume 5, Issue 8, pp 20-26, August 2026
ISSN (Online): 2583-7257
Article DOI: https://doi.org/10.47001/ICJES/2026.508003

Material Characterization of Diesel Engine Connecting Rod Excavator 6 Cylinder 350 HP

[1]*Parant Widiyono, [2]Sulardjaka, [3]Agus Suprihanto

[1,2,3]Mechanical Engineering Department, Faculty of Engineering, Diponegoro University, Jl. Prof. H. Soedarto, SH, Tembalang-Semarang 50275, Indonesia
*Corresponding Author's E-Mail: parantw@gmail.com

***Abstract* - Component failures in heavy equipment engines can cause significant operational losses, particularly in the mining industry. One of the critical components in an excavator diesel engine is the connecting rod, which functions to transmit combustion forces from the piston to the crankshaft. This study aims to analyze the mechanism and causes of connecting rod failure in a 6-cylinder 350 HP excavator engine that experienced permanent deformation. The methods employed include visual observation, chemical composition testing, metallographic examination, Vickers hardness testing. Test results indicate that the connecting rod material conforms to OEM specifications, namely AISI 1548 steel with a ferrite–pearlite microstructure and an average hardness of 245 HV. However, maintenance history investigation revealed that overheating occurred, causing cylinder head gasket failure and liner deformation, which allowed coolant to enter the combustion chamber. This condition triggered the hydro lock phenomenon, generating extreme pressure that exceeded the connecting rod design capacity and resulting in buckling failure. The findings of this study confirm that the failure was not caused by material defects or design flaws, but rather by abnormal operating conditions, and provide a technical basis for preventing similar failures in heavy equipment diesel engines.**

Keywords: Connecting rod, hydro lock, buckling, material characterization.

I. INTRODUCTION

The connecting rod is one of the primary components in an internal combustion engine, functioning to transmit combustion forces from the piston to the crankshaft, thereby converting translational motion into rotational motion [1]. In diesel engines, particularly those of heavy equipment, the connecting rod operates under a combination of compressive, tensile, and bending loads that are dynamic and repetitive throughout the engine operating cycle [2]. This makes the connecting rod a highly critical component with respect to engine reliability and service life.

Connecting rod failure can cause serious engine damage, even leading to complete operational shutdown, resulting in significant economic losses [3]. Various previous studies have reported that connecting rod failures are generally caused by fatigue mechanisms due to high cyclic loading, stress concentration in critical areas, material defects, as well as design and manufacturing errors [4][5]. Analytical methods commonly used in these studies include visual observation, metallographic testing, mechanical property testing, and numerical simulation using the finite element method to evaluate stress distribution and safety factors [6][7][2].

In addition to failures under normal operating conditions, several studies have also reported connecting rod failures caused by abnormal operating conditions, one of which is the hydro lock phenomenon [8]. Hydro lock occurs when liquid enters the combustion chamber such that the piston cannot perform the compression stroke normally, resulting in a drastic pressure increase that loads the connecting rod beyond its design capacity [8]. This condition can potentially cause permanent plastic deformation or buckling failure [9].

Nevertheless, most previous studies have focused on material fatigue failures, while investigations of connecting rod failure due to hydro lock that integrate material analysis, buckling simulation, and engine operating history—particularly in excavator diesel engines—remain limited. Therefore, this study aims to analyze connecting rod failure in a 6-cylinder 350 HP excavator engine through a comprehensive approach encompassing visual observation, chemical composition testing, metallographic examination, hardness testing, and numerical analysis using the finite element method, in order to accurately identify the failure mechanism and primary cause.

II. METHODS

The connecting rod experienced failure as shown in Figure 1, exhibiting buckling with evidence of bending deformation at the shank area.

International Current Journal of Engineering and Science (ICJES)
Volume 5, Issue 8, pp 20-26, August 2026
ISSN (Online): 2583-7257
Article DOI: https://doi.org/10.47001/ICJES/2026.508003

Figure 1: Connecting Rod

This study commenced with visual observation of the connecting rod and the cylinder head area, followed by hardness testing, microstructure, chemical composition testing.

2.1 Hardness Testing

Hardness testing was conducted in accordance with ASTM E18. The test was performed by sectioning the buckling area, specifically at the region of maximum bending in the connecting rod. The testing equipment used was the Vickers hardness tester HMV-2000. Measurement points were taken starting from 0.5 mm from the outermost wall of the connecting rod cross-section to the central area, as illustrated in Figure 2.

2.2 Chemical Composition Testing

Chemical composition testing was conducted to determine the amount and weight percentage of elemental constituents in the connecting rod material. Testing was performed on the failed connecting rod and compared with an OEM connecting rod. Chemical composition analysis was carried out using a Foundry Master optical emission spectrometer.

2.3 Microstructure Observation

Microstructure examination was performed on both the failed material and the OEM part. The process began with sectioning at the area of maximum deformation, followed by grinding up to grit 5000. The polished and lustrous surface was then etched with 2% Nital solution. After etching, the specimens were observed using an Olympus BX 41M optical microscope at magnifications of 200X and 500X, focusing on the outermost and inner areas of the connecting rod.

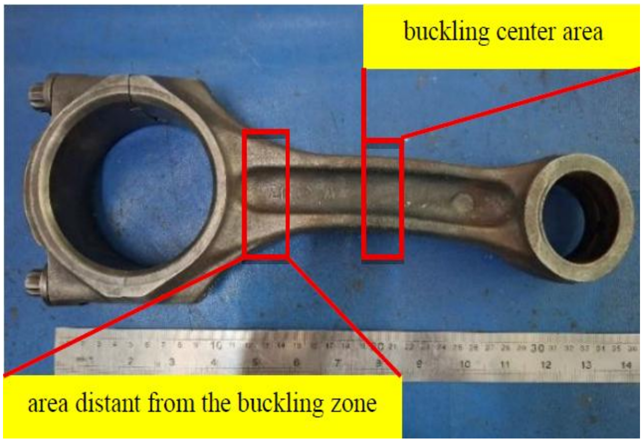

(a)

(b)

Figure 2: a) Sample cutting area for test specimen preparation b) Hardness test point locations from the surface to the center of the part

III. RESULTS AND DISCUSSIONS

3.1 Hardness Test Result

Figures 3 and 4 present the hardness results of specimens at the buckling center and the area distant from the buckling zone, respectively. The results indicate that the hardness at the edge area is higher than at the interface and center regions, reaching 298 HV. The maximum hardness value for AISI 1548 material ranges between 230–270 HV thus, the hardness value at the buckling center exceeds this standard. This is attributed to plastic deformation at the outermost diameter of the material, which increased the local hardness value.

International Current Journal of Engineering and Science (ICJES)
Volume 5, Issue 8, pp 20-26, August 2026
ISSN (Online): 2583-7257
Article DOI: https://doi.org/10.47001/ICJES/2026.508003

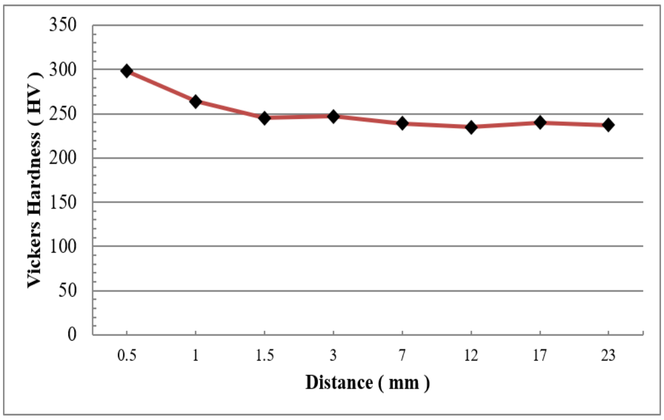

Figure 3: Hardness profile at the buckling area

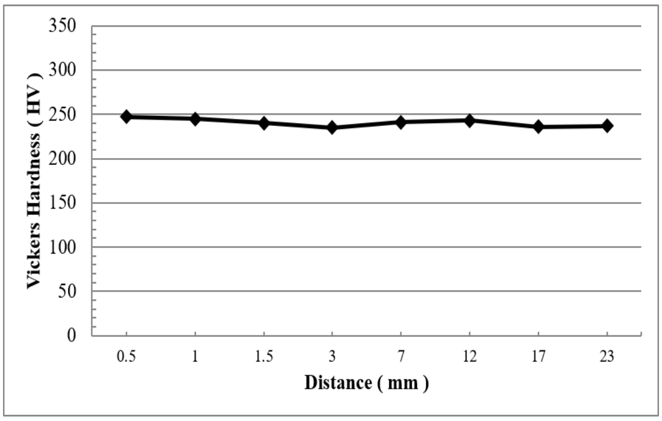

Figure 4: Hardness profile at the area distant from the buckling zone

As reported in previous studies, the bending process causes an increase in hardness at the outer dimension area, with hardness values gradually approaching those of the original material toward the interior [10].The localized increase in hardness observed at the outermost region of the buckling section also provides indirect evidence that the connecting rod experienced severe plastic deformation rather than thermal degradation. During hydro lock, the connecting rod is subjected to a compressive load exceeding its yield strength, causing localized plastic strain at the outer fibers where bending stress reaches its maximum.

The accumulation of plastic strain increases the dislocation density within the ferrite matrix, thereby restricting dislocation mobility and producing a strain-hardening effect. Consequently, the hardness increases significantly near the outer surface while gradually decreasing toward the neutral axis where plastic strain is minimal. This hardness gradient is characteristic of cold-worked steel subjected to bending deformation and confirms that the observed hardness increase is a consequence of overload-induced deformation instead of changes in chemical composition or heat treatment. Similar strain-hardening behavior has been reported for bent carbon steel components where the increase in Vickers hardness was directly correlated with local plastic strain and dislocation accumulation [10]. The hardness in areas distant from the buckling center remains within the standard range of 235–245 HV, as seen in Figure 3, and similarly the OEM connecting rod exhibits hardness values between 240–247 HV as shown in Figure 5.

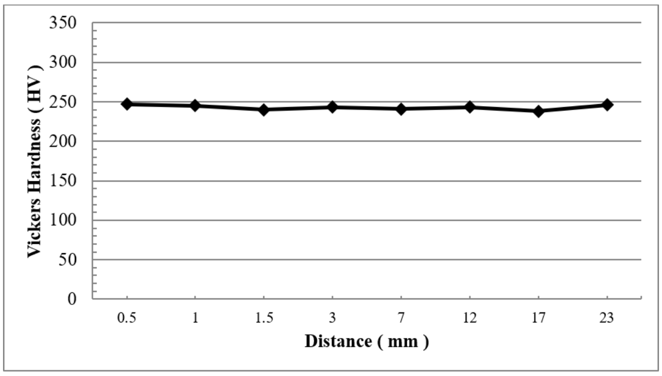

Figure 5: Hardness profile of the OEM connecting rod

3.2 Chemical Composition Test Results

The connecting rod material used in this excavator diesel engine is a high-manganese carbon steel, with a carbon content of 0.48 wt% and a manganese content of 1.15 wt%, equivalent to AISI 1548. The chemical composition test results comparing the failed part with the OEM part are presented in Table 1.

Table 1: OEM Chemical Composition Test Results Failed Part vs. OEM Part

Element	Part Failure	Part OEM
Iron Fe	97.6	98.5
Carbon C	0.480	0.519
Mangan Mn	1.150	1.130
Phosphor P	0.019	0.010
Sulfur S	0.044	0.041

The test results show no significant difference in chemical composition between the failed part and the OEM part. Compared to the standard chemical composition, both conform to AISI 1548 specifications as shown in Table 2.

International Current Journal of Engineering and Science (ICJES)
Volume 5, Issue 8, pp 20-26, August 2026
ISSN (Online): 2583-7257
Article DOI: https://doi.org/10.47001/ICJES/2026.508003

Table 2: AISI 1548 Chemical Composition Standard

Element	AISI 1548 Standard
Iron Fe	97.0 – 98.5
Carbon C	0.44 – 0.52
Mangan Mn	1.10 – 1.40
Phosphor P	Max 0.04
Sulfur S	Max 0.05

Based on the identified material as AISI 1548, the mechanical properties of the connecting rod material can be determined, as presented in Table 3.

Table 3: Mechanical Properties of the Connecting Rod Material

Element	AISI 1548 Standard
Tensile Strength (Mpa)	750 - 950
Yield Strength (Mpa)	600 – 780
Modulus of Elasticity (GPa)	210
Poison Ratio	0.29 – 0.30
Elongation (%)	10 - 14
Hardness (HV)	230 – 270

3.3 Microstructure Test Results

Microstructure examination using the Olympus BX41M optical microscope reveals that the connecting rod material consists of ferrite and pearlite phases, which is consistent with the characteristics of AISI 1548 material, as shown in Figure 6.

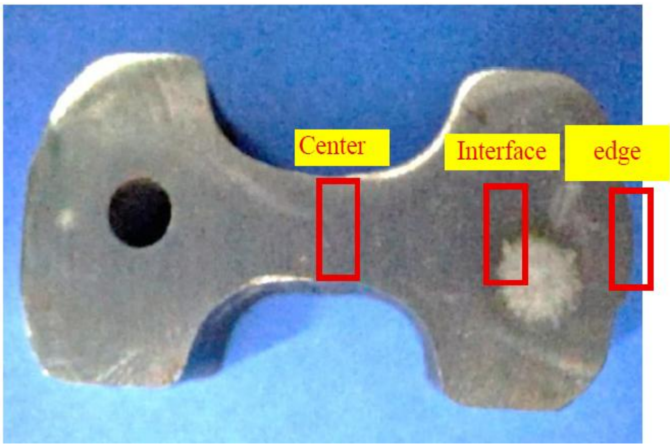

(a)

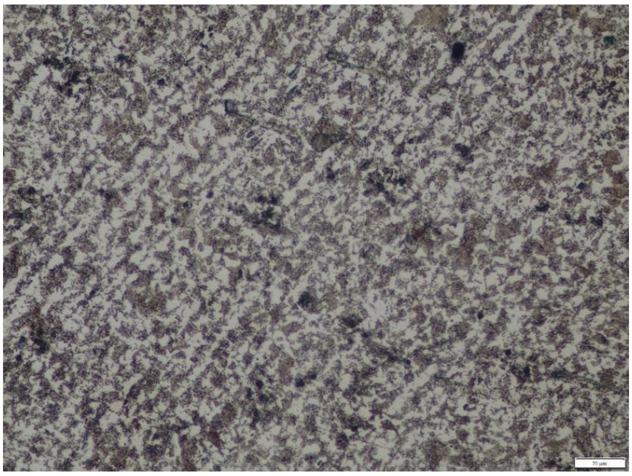

(b)

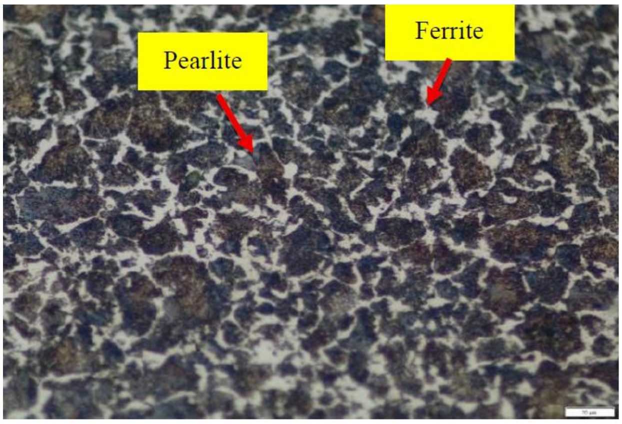

(c)

Figure 6: a) Microstructure sampling area b) Microstructure at the edge area at 500X magnification c) Microstructure at the interface and center area at 500X magnification

From the microstructure results in Figure 6b, it can be observed that at the outermost point (edge) of the buckling center, the microstructure has become flattened and elongated due to deformation caused by buckling. This is also consistent with findings from previous studies, which indicate that during the bending process, the microstructure at the outer side of the material becomes flatter compared to that of the center region [11], also shows the microstructure at the outer edge of the buckling region, where the connecting rod experienced the highest compressive-bending strain during the hydro lock event. The microstructure consists of ferrite (light phase) and pearlite (dark lamellar colonies), which is characteristic of normalized AISI 1548 medium-carbon steel. Compared with the undeformed region, both ferrite grains and pearlite colonies exhibit noticeable elongation and flattening along the deformation direction, indicating severe plastic deformation after the applied compressive stress exceeded the material yield strength.

Volume 5, Issue 8, pp 20-26, August 2026
ISSN (Online): 2583-7257
Article DOI: https://doi.org/10.47001/ICJES/2026.508003

This morphological change is attributed to the accumulation and movement of dislocations within the ferrite matrix, causing grains to elongate while pearlite colonies rotate and align parallel to the principal strain direction. Such grain distortion is a typical microstructural response during cold plastic deformation and bending, where the outermost fibers experience the maximum equivalent plastic strain. Importantly, no evidence of microcracks, intergranular fracture, carbide fragmentation, abnormal inclusions, or phase transformation was observed, indicating that the metallurgical integrity of the material remained intact despite the severe deformation. This observation confirms that the microstructural modification resulted from mechanical overload rather than manufacturing defects or improper heat treatment. Furthermore, the elongated ferrite–pearlite morphology is consistent with the localized hardness increase observed at the same region, since plastic deformation increases dislocation density and produces strain hardening, thereby increasing the resistance of the material to further plastic flow. Similar deformation-induced grain elongation and hardness enhancement in bent steel components have been reported by [10], while [11] demonstrated that the degree of grain distortion is directly associated with the distribution of plastic strain across the bent cross-section. These observations strongly support the conclusion that the connecting rod failure was governed by overload-induced plastic buckling caused by hydro lock rather than by metallurgical degradation.

Figure 6c presents the microstructure observed at the center region of the connecting rod cross-section, corresponding to the neutral axis of the buckled section. The microstructure consists of a typical ferrite–pearlite structure, where ferrite appears as the bright phase and pearlite as the darker lamellar colonies. Unlike the edge region, no evidence of grain elongation or phase flattening is observed, indicating that this region did not experience significant plastic deformation during the buckling event. The ferrite grains retain their equiaxed morphology, while the pearlite colonies remain uniformly distributed with random orientation, suggesting that the original metallurgical structure was preserved. According to the mechanics of bending, the neutral axis undergoes negligible longitudinal strain, whereas the maximum tensile and compressive strains are concentrated at the outermost fibers of the cross-section. Consequently, the center region experiences only elastic deformation, resulting in minimal dislocation multiplication and no appreciable strain hardening or microstructural distortion. Furthermore, no metallurgical discontinuities such as microcracks, voids, carbide fragmentation, abnormal inclusions, or phase transformation were detected, confirming that the material maintained its metallurgical integrity throughout the loading process. This observation is consistent with the hardness profile measured in the same region, where the hardness remained within the standard range for AISI 1548 steel (approximately 235–245 HV), indicating that the increase in hardness was localized only at the outer buckling surface. Similar microstructural behavior has been reported by [11], who demonstrated that deformation during bending is concentrated in the outer fibers, while the microstructure near the neutral axis remains essentially unchanged. Likewise, [10] showed that plastic strain and strain hardening decrease progressively from the outer surface toward the center of a bent steel section, producing a corresponding gradient in both microstructural deformation and hardness. Therefore, the preserved ferrite–pearlite morphology at the center region provides further evidence that the connecting rod failure resulted from localized overload-induced plastic buckling associated with the hydro lock phenomenon, rather than from intrinsic metallurgical defects or material degradation.

VI. CONCLUSION

This study comprehensively investigated the failure mechanism of a connecting rod from a 350 HP six-cylinder excavator diesel engine through visual inspection, chemical composition analysis, Vickers hardness testing, and metallographic examination. The results confirmed that the connecting rod material complies with the specifications of AISI 1548 medium-carbon manganese steel, exhibiting a homogeneous ferrite–pearlite microstructure and chemical composition consistent with the OEM component. No evidence of metallurgical defects, material degradation, abnormal inclusions, microcracks, or improper heat treatment was identified, indicating that the material possessed adequate metallurgical quality and mechanical properties prior to failure.

Hardness measurements revealed a localized increase to approximately 298 HV at the outer edge of the buckled section, whereas the center region maintained the standard hardness range of 235–245 HV. This hardness gradient corresponds to the distribution of plastic strain generated during buckling, where the outer fibers experienced severe strain hardening due to dislocation accumulation while the neutral axis remained largely unaffected. Metallographic observations further confirmed this behavior by revealing elongated ferrite–pearlite morphology in the edge region, whereas the center retained its original equiaxed microstructure without evidence of significant plastic deformation. The excellent agreement between the hardness profile and microstructural evolution demonstrates that the observed metallurgical changes were deformation-induced rather than the result of material deficiencies.

Volume 5, Issue 8, pp 20-26, August 2026
ISSN (Online): 2583-7257
Article DOI: https://doi.org/10.47001/ICJES/2026.508003

Based on the combined experimental evidence and maintenance history, it is concluded that the connecting rod failure was governed by localized plastic buckling caused by an overload condition associated with the hydro lock phenomenon. The excessive compressive force generated by incompressible coolant trapped inside the combustion chamber exceeded the yield strength of the connecting rod, producing permanent plastic deformation without initiating conventional fatigue failure. Therefore, the primary root cause of failure was abnormal engine operating conditions rather than deficiencies in material selection, manufacturing quality, or component design.

The findings of this study provide important practical implications for heavy-duty diesel engine maintenance by emphasizing that early detection of cooling system failures, cylinder head gasket leakage, and liner deformation is essential to prevent coolant ingress into the combustion chamber and subsequent hydro lock. Furthermore, this integrated failure analysis demonstrates the importance of combining metallurgical characterization with service history to accurately distinguish overload-induced failures from failures caused by material defects, thereby improving the reliability of failure diagnosis and maintenance strategies for heavy equipment engines.

REFERENCES

[1] G. Shanmugasundar, M. Dharanidharan, D. Vishwa, and A. P. Sanjeev Kumar, “Design, analysis and topology optimization of connecting rod,” *in Materials Today: Proceedings, Elsevier Ltd*, 2020, pp. 3430–3438. doi: 10.1016/j.matpr.2020.11.778.

[2] Z. Zhang, A. Jiao, X. Lv, and H. Ding, “Study of failure analysis and manufacturing processes improvement of cracking connecting rod,” *Journal of Mechanical Science and Technology*, vol. 36, no. 11, pp. 5445–5453, Nov. 2022, doi: 10.1007/s12206-022-1010-0.

[3] A.Artigas, A. Monsalve, R. Colás, and N. F. Garza-Montes-de-Oca, “Failure analysis of the fasten system of wheels used in mining pickup trucks,” *Case Stud. Eng. Fail. Anal.*, vol. 8, pp. 28–35, Apr. 2017, doi: 10.1016/j.csefa.2017.02.001.

[4] L. Witek and P. Zelek, “Stress and failure analysis of the connecting rod of diesel engine,” *Eng. Fail. Anal.*, vol. 97, pp. 374–382, Mar. 2019, doi: 10.1016/j.engfailanal.2019.01.004.

[5] H. Zhou, S. Liu, G. Li, G. Tian, Z. Wang, and C. Wang, “Machining Stress Analysis and Deformation Prediction of Connecting Rod Based on FEM and GRNN,” *Iranian Journal of Science and Technology - Transactions of Mechanical Engineering*, vol. 44, no. 1, pp. 183–192, Mar. 2020, doi: 10.1007/s40997-018-0256-8.

[6] O. K. Ajayi, B. O. Malomo, S. D. Paul, A. A. Adeleye, and S. A. Babalola, “Failure modeling for titanium alloy used in special purpose connecting rods,” *in Materials Today: Proceedings, Elsevier Ltd*, 2021, pp. 4390–4397. doi: 10.1016/j.matpr.2020.11.852.

[7] Z. Shi and S. Kou, “Inverse Reconstruction of Fracture Splitting Connecting Rod and its Strength and Fatigue Life,” *Journal of Failure Analysis and Prevention*, vol. 18, no. 3, pp. 619–627, Jun. 2018, doi: 10.1007/s11668-018-0450-4.

[8] M. A. Rezvani, D. Javanmardi, and P. Mostaghim, “Diagnosis of EMD645 diesel engine connection rod failure through modal testing and finite element modeling,” *Eng. Fail. Anal.*, vol. 92, pp. 50–60, Oct. 2018, doi: 10.1016/j.engfailanal.2018.05.005.

[9] A.R. Pani, R. K. Patel, and G. K. Ghosh, “Buckling analysis and material selection of connecting rod to avoid hydro-lock failure,” *Materials Today: Proceedings*, vol. 27, pp. 2121–2126, 2019, doi: 10.1016/j.matpr.2019.09.079.

[10] C. LIU, A. IWASAKI, and W. LIN, “A fundamental study on the hardness-strain in bent cross-section of thin steel panels during the hemming process with a comparison between experimental and numerical approach,” *Mechanical Engineering Journal*, vol. 11, no. 1, pp. 23-00256-23–00256, 2024, doi: 10.1299/mej.23-00256.

[11] F. Niu, J. He, D. Liu, X. Zuo, and M. Cai, “Effect of Bending Process on Microstructure, Mechanical Properties and Crack Formation of 5% Ni Steel,” *Metals (Basel).*, vol. 12, no. 7, Jul. 2022, doi: 10.3390/met12071188.

International Current Journal of Engineering and Science (ICJES)

Volume 5, Issue 8, pp 20-26, August 2026

ISSN (Online): 2583-7257

Article DOI: https://doi.org/10.47001/ICJES/2026.508003

Citation of this Article:

Parant Widiyono, Sulardjaka, & Agus Suprihanto. (2026). Material Characterization of Diesel Engine Connecting Rod Excavator 6 Cylinder 350 HP. *International Current Journal of Engineering and Science (ICJES)*, 5(8), 20-26. Article DOI: https://doi.org/10.47001/ICJES/2026.508003

****